

Exceptionally Low Thermal Conductivities of Films of the Fullerene Derivative PCBM

John C. Duda and Patrick E. Hopkins*

Department of Mechanical and Aerospace Engineering, University of Virginia, Charlottesville, Virginia 22904, USA

Yang Shen and Mool C. Gupta†

Department of Electrical and Computer Engineering, University of Virginia, Charlottesville, Virginia 22904, USA

(Received 25 May 2012; revised manuscript received 30 October 2012; published 2 January 2013)

We report on the thermal conductivities of microcrystalline [6,6]-phenyl C₆₁-butyric acid methyl ester (PCBM) thin films from 135 to 387 K as measured by time domain thermorefectance. Thermal conductivities are independent of temperature above 180 K and less than $0.030 \pm 0.003 \text{ W m}^{-1} \text{ K}^{-1}$ at room temperature. The longitudinal sound speed is determined via picosecond acoustics and is found to be 30% lower than that in C₆₀/C₇₀ fullerite compacts. Using Einstein's model of thermal conductivity, we find the Einstein characteristic frequency of microcrystalline PCBM is $2.88 \times 10^{12} \text{ rad s}^{-1}$. By comparing our data to previous reports on C₆₀/C₇₀ fullerite compacts, we argue that the molecular tails on the fullerene moieties in our PCBM films are responsible for lowering both the apparent sound speeds and characteristic vibrational frequencies below those of fullerene films, thus yielding the exceptionally low observed thermal conductivities.

DOI: [10.1103/PhysRevLett.110.015902](https://doi.org/10.1103/PhysRevLett.110.015902)

PACS numbers: 66.70.-f, 63.22.-m, 65.80.-g

As a field of study, thermal transport is both ubiquitous and pervasive, as many technologies face a thermal management challenge at some point in their lifetimes [1]. Beyond application, the topic of thermal conductivity of the solid state has long been one of general scientific interest [2–4], and a large and ongoing effort has been set forth to expanding the limits of heat conduction [5,6]. On one end of the spectrum, the so called “lower limit” of thermal conductivity is typically observed in amorphous phases of materials, where conductivities are much lower compared to that of their single crystalline counterparts [7]. In these phases, heat conduction is described by a random walk of vibrational energy on the time and length scales of atomic vibrations and interatomic spacing, respectively [2,8]. In addition, one can approach this lower limit by creating multilayer, nano-crystalline, or porous films in which the spacing between interfaces, grain boundaries, or pores is on the order of several nanometers [9–16]. In these nanostructured materials, boundaries impede thermal transport by scattering phonons, thereby shortening their mean-free paths and yielding lower thermal conductivities.

Yet another advantage of nanostructuring is the possibility of creating an amorphouslike network of large, repeating unit cells. In such materials, low thermal conductivities can be realized not only by limiting phonon mean-free paths, but also through the localization of vibrations. For example, the low thermal conductivities of compacted C₆₀/C₇₀ fullerite microcrystals reported by Olson and Pohl [17] were attributed to the largely independent and poorly coupled oscillations within each of the fullerenes. This explanation was further supported by low temperature heat capacity measurements that demonstrated Einstein-like behavior despite the microcrystallinity of

the compacts. More recently, Chiretescu *et al.* [18] reported a large reduction in the thermal conductivity of a homogeneous solid through growth of layered WSe₂, in which weak interlayer bonding led to a decrease in thermal conductivity below that of a single crystal of WSe₂ along the *c* axis by a factor of thirty, and below the corresponding theoretical minimum limit by a factor of six. There, too, the authors noted that localization of vibrations could be partly responsible for the observed behavior.

In this Letter, we report on thermal conductivities of the fullerene derivative [6,6]-phenyl C₆₁-butyric acid methyl ester (PCBM) from 135 to 387 K. Thermal conductivities of PCBM thin films were measured via time-domain thermorefectance (TDTR), a noncontact, pump-probe optical thermometry technique. Above 180 K, thermal conductivities were independent of temperature and less than $0.030 \pm 0.003 \text{ W m}^{-1} \text{ K}^{-1}$, a factor of three less than that of C₆₀/C₇₀ fullerite microcrystals [17]. In addition, no significant dependence on the type of substrate on which the film was deposited, subsequent heat treatment, or film thickness over the range 22 to 106 nm was observed. Microcrystallinity was confirmed by transmission electron microscopy and electron beam diffraction. As with the aforementioned works, we attribute these exceptionally low thermal conductivities to highly localized vibrations with low characteristic frequencies, as well as low longitudinal sound speeds ($2300 \pm 100 \text{ m s}^{-1}$ as measured by picosecond acoustics, $\approx 30\%$ lower than those measured in compacted C₆₀/C₇₀ fullerite microcrystals). Last, we note these films exhibit the lowest reported room-temperature thermal conductivity of any fully dense solid [6,18].

PCBM thin films were prepared according to the following procedure: indium tin oxide (ITO) coated glass

substrates (provided by Delta Technologies) were first cleaned with acetone and isopropyl alcohol and subsequently dried with air. Highly conductive PEDOT:PSS provided by H.C. Starck was then spin cast on these substrates from aqueous solution. The PEDOT:PSS films had average thicknesses of near 60 nm, and were baked for 15 min at 110 °C in air. PCBM (provided by Sigma-Aldrich) was dissolved in chlorobenzene at 1 wt% for 24 h before fabrication and subsequently spin cast on the substrates at various speeds, creating films ranging in thickness from 22 to 106 nm as measured by profilometry. A set of these films were set aside, while others were annealed in air at 130 °C for 2 min. The surface morphology of each film was measured by atomic force microscopy. A nominally 80 nm thick Al film was then deposited on the films (including on the PEDOT:PSS reference sample) via electron beam evaporation to serve as a transducer for the thermal measurement. The electrical resistivities of films prepared in identical fashion were measured via a procedure we outlined previously [19], where the cross-plane resistivity was determined to be $3.1 \times 10^6 \Omega \text{ cm}$. In agreement with the literature reporting on the structure of PCBM films processed via chlorobenzene solution [20,21], the observation of distinct rings in the diffraction pattern generated by electron beam diffraction (shown in Fig. 1) confirmed the microcrystallinity of the films. As one might expect, the diffraction patterns also indicate that annealing lead to further crystallization.

The thermal conductivities and longitudinal sound speeds of these fullerene-derivative films were measured with TDTR [22,23]. Time-domain thermorefectance and appropriate analyses accounting for pulse accumulation when using a Ti:sapphire oscillator have been detailed previously by several groups [14,24–26]. In short, TDTR is a pump-probe technique in which 100 fs laser pulses emanate from a Spectra Physics Tsunami at an 80 MHz repetition rate. We delay the time in which the probe pulse reaches the sample relative to the pump pulse by way of a mechanical delay stage (for a maximum delay of ≈ 6.0 ns). In this study, we modulate the pump at 11.39 MHz and monitor the ratio of the in-phase to

out-of-phase signal of the probe beam from a lock-in amplifier ($-V_{\text{in}}/V_{\text{out}}$, and example data are shown in the inset of Fig. 2). Our pump and probe spots are focused to $1/e^2$ radii of 25 and 6 μm at the sample surface, respectively; at these sizes and at the 11.39 MHz pump modulation frequency we are negligibly sensitive to any in-plane transport in the films, thus decreasing the uncertainty associated with determining the cross-plane thermal conductivity [27,28]. We take a total of six TDTR measurements on each film at temperatures from 135 to 387 K in a cryostat with optical access that is kept under vacuum (<1.0 mTorr) [29]. We limit the total incident laser power to ≤ 30 mW in order to minimize steady-state heating of the samples; still, due to the low thermal conductivity of our thermal sink (glass) the temperature rise due to the incident beams is ≈ 25 K at room temperature [24]. We add the calculated steady-state temperature rise at each set point to the cryostat temperature and use this temperature in our subsequent analysis.

We fit the TDTR data with a thermal model that accounts for pulse accumulation in a layered system. At our modulation frequency, we are sensitive to thermal effusivity, $\sqrt{\kappa C}$, where κ is the thermal conductivity and C is the volumetric specific heat [24,30]. Consequently, in order to determine thermal conductivities, the volumetric specific heats must be known. We assume literature values for the specific heat of the Al [31] and approximate the specific heat of PCBM from data on C_{60}/C_{70} fullerite

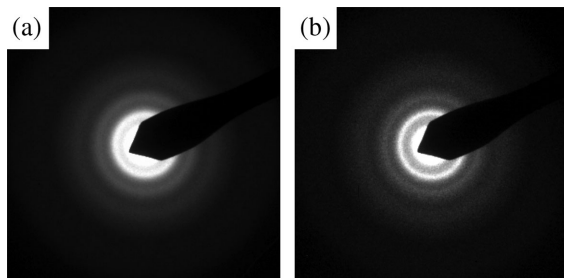


FIG. 1. Electron diffraction patterns of (a) unannealed and (b) annealed PCBM films. Note the rings in diffraction pattern from the annealed sample are more distinct than they are in the unannealed sample, indicating an increase in crystallinity.

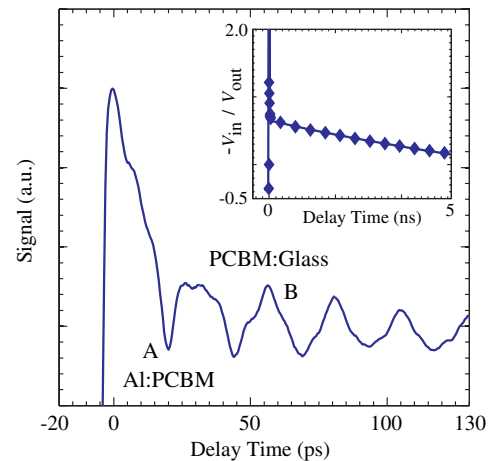


FIG. 2 (color online). Picosecond acoustics data taken on a 68 nm Al transducer on a 39 nm PCBM film coated on glass. The time between the initial peak and the trough due to the reflection at the Al:PCBM interface (labeled “A”) is used to confirm the Al transducer thickness. The time between the trough at A and the peak due to the reflection from the PCBM:glass interface (labeled “B”) is used to determine the longitudinal sound speed in the PCBM film. Averaging measurements made on several samples of varying thickness yielded a longitudinal sound speed of $2300 \pm 100 \text{ m s}^{-1}$. The inset shows example data from TDTR measurements on a 74 nm PCBM film (closed symbols) and the corresponding thermal model (solid line).

microcrystals (Ref. [17]), as they exhibit a very similar crystal structure to PCBM films processed via chlorobenzene solution (both exhibit fcc-like lattices with a center-to-center distance between fullerene moieties of ≈ 10 Å) [20,21]. This assumption is made on the side of caution; by effectively ignoring the molecular tail, we are underestimating the specific heat, and thus overestimating the conductivity (i.e., the thermal conductivities may be, in fact, slightly lower than we report). However, since these molecular tails primarily contribute high-frequency modes, e.g., C-H stretching, they are likely “frozen out” at the temperatures considered in the present study (as determined by Bose-Einstein statistics).

The thermal conductivity of the Al is approximated from previous measurements of electrical resistivity of evaporated Al thin films via the Wiedemann-Franz law [26], although we are relatively insensitive to the Al layer during the time span of our TDTR measurements. The exact thicknesses of the Al films are confirmed via picosecond acoustics [32,33]. Finally, despite the relative thinness of the polymer films, their thermal conductivities are low enough that we are not sensitive to the underlying layers of or interfaces between PEDOT:PSS, ITO, or the substrate at our modulation frequency. This is confirmed by appropriate sensitivity analyses [34] and by the fact we observe no dependence of the measured thermal conductivities on the film thicknesses (as will be discussed below). This leaves the thermal conductivity of the PCBM film as the only free parameter in the model.

The measured thermal conductivities of the PCBM thin films are plotted as a function of temperature in Fig. 3(a) and as a function of film thickness in 3(b). In addition, we plot the thermal conductivities of amorphous carbon from Ref. [35], C_{60}/C_{70} fullerite microcrystals from Ref. [17], phosphorus-doped C_{60} from Ref. [36], and layered WSe_2 from Ref. [18]. Last, for comparison, we also calculate the theoretical minimum thermal conductivity, κ_{\min} , of C_{60}/C_{70} fullerite microcrystals and PCBM as proposed by Ref. [8],

$$\kappa_{\min} = \left(\frac{\pi}{6}\right)^{1/3} k_B n^{2/3} \sum_{i=1}^3 v_i \left(\frac{T}{\Theta_i}\right)^2 \int_0^{\Theta_i/T} \frac{x^3 e^x}{(e^x - 1)^2} dx, \quad (1)$$

where i is the polarization index, k_B is the Boltzmann constant, v_i is the polarization-specific sound speed (longitudinal, L , or transverse, T), n is the atomic density, and $\Theta_i = v_i(\hbar/k_B)(6\pi^2 n)^{1/3}$ is the cutoff frequency expressed in units K. This model assumes that the lifetimes of the Debye-like, heat-carrying oscillations are one half the period of vibration (i.e., the mean-free-paths are half the corresponding wavelengths) [8]. For our C_{60}/C_{70} calculations, sound speeds were measured by ultrasonic measurements ($v_L = 3300$ m s $^{-1}$, $v_T = 1900$ m s $^{-1}$) and atomic density was determined via x-ray diffraction ($n = 8.78 \times 10^{22}$ cm $^{-3}$), as reported in Ref. [17]. For

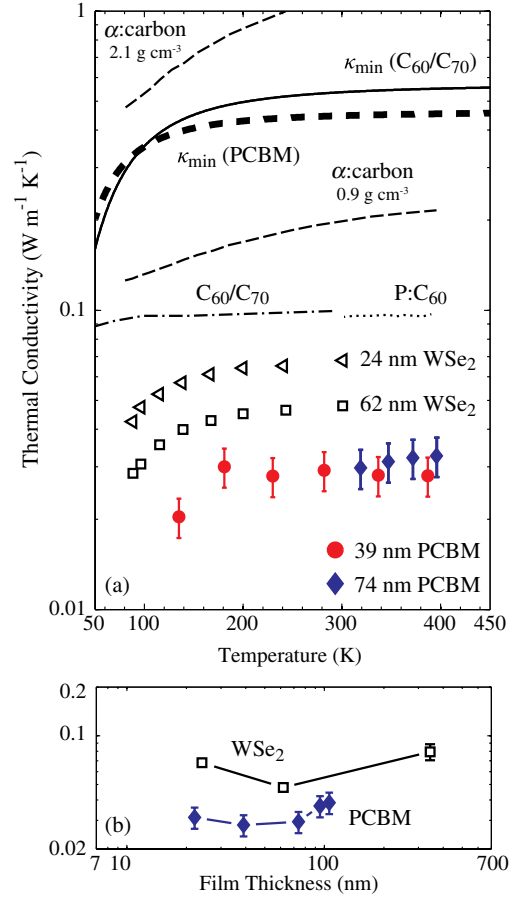


FIG. 3 (color online). (a) The measured thermal conductivities of 39 and 74 nm PCBM films, along with previously published thermal conductivities of amorphous carbon films, (light dashed lines, Ref. [35]), C_{60}/C_{70} fullerite microcrystals (dash-dot line, Ref. [17]), phosphorus-doped C_{60} (dotted line, Ref. [36]), and layered WSe_2 (hollow symbols, Ref. [18]). The solid line represents the theoretical minimum thermal conductivity of a disordered C_{60}/C_{70} crystal as predicted by Eq. (1), and the heavy dashed line the equivalent for PCBM. Error bars represent the repeatability of the measurement on each sample in addition to the sensitivity to a ± 2 nm change in Al transducer thickness. (b) Measured thermal conductivities of PCBM films as a function of film thickness.

PCBM, the longitudinal sound speed was measured from picosecond acoustics ($v_L = 2300$ m s $^{-1}$, see example data in Fig. 2) and the transverse was scaled based on longitudinal to transverse ratio in C_{60}/C_{70} ($v_T = 1325$ m s $^{-1}$). Atomic density of the PCBM was calculated based on the observed structure of films processed via chlorobenzene solution ($n = 1.26 \times 10^{23}$ cm $^{-3}$) [20,21]. Finally, singly degenerate longitudinal and doubly degenerate transverse polarizations were assumed.

The thermal conductivities of PCBM films as reported in Figs. 3(a) and 3(b) are nearly a factor of three lower than those of C_{60}/C_{70} fullerite microcrystals and up to a factor of two lower than that of layered WSe_2 . In addition, the thermal conductivities of PCBM are independent of

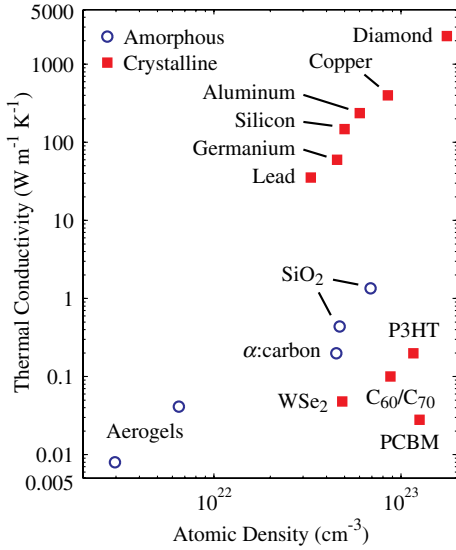


FIG. 4 (color online). Room-temperature thermal conductivity of various materials plotted as a function of their atomic density. The values for diamond, copper, aluminum, silicon, germanium, and lead are from Ref. [31], SiO₂ and aerogels from Ref. [16], amorphous carbon from Ref. [35], WSe₂ from Ref. [18], C₆₀/C₇₀ from Ref. [17], P3HT from Ref. [38] and PCBM is from the present work. Not only does PCBM exhibit the lowest conductivity, but it is among the densest of the materials, second only to diamond.

temperature between 180 and 387 K and largely insensitive to film thickness in the range 22 to 106 nm as shown in Fig. 3(b). We also note that the chosen substrate (additional films were deposited on glass and silicon, as opposed to the ITO and PEDOT:PSS coated glass slides described above) or heat treatment (annealed or unannealed) did not lead to statistically significant changes in thermal conductivity.

In Ref. [17], Olson and Pohl used low temperature heat capacity measurements to determine the Einstein temperature of C₆₀/C₇₀ fullerite microcrystals, $\Theta_E = 35$ K, which corresponds to a frequency of $k_B \Theta_E / \hbar = 4.58 \times 10^{12}$ rad s⁻¹, where \hbar is Planck's constant divided by 2π . With this value and the Einstein model of thermal conductivity,

$$\kappa_E = 2 \frac{k_B^2}{\hbar} \frac{N^{1/3}}{\pi} \Theta_E \frac{x^2 e^x}{(e^x - 1)^2}, \quad (2)$$

where N is the fullerene density and $x = \Theta_E/T$, they found excellent agreement between the model and their data. Following the reverse procedure and fitting the Einstein model of thermal conductivity to our temperature-dependent thermal conductivity data yields $\Theta_E = 22$ K, which corresponds to a frequency of 2.88×10^{12} rad s⁻¹. This suggests that the presence of the molecular tail is not only responsible for lowering the sound speeds of PCBM microcrystals, but also lowering the characteristic frequency of their highly localized vibrations.

To put the exceptionally low thermal conductivity of PCBM into perspective, in Fig. 4, we plot the room-temperature thermal conductivities of several amorphous and crystalline materials as a function of their atomic density. While previous reports have made similar comparisons with regard to mass density [6], plotting thermal conductivity as a function of atomic density allows easier identification of trends among crystalline and amorphous materials, respectively. The outliers (P3HT, C₆₀/C₇₀, and PCBM) are nominally microcrystalline, exhibit some of the highest atomic densities, and simultaneously, some of the lowest conductivities. In this respect, it is interesting to note that some of the best thermal conductors, as well as the best thermal insulators, are carbon allotropes or carbon based materials [37].

In summary, we have reported on the thermal conductivities of [6,6]-phenyl C₆₁-butyric acid methyl ester (PCBM) thin films from 135 to 387 as measured by time domain thermoreflectance. Thermal conductivities were shown to be independent of temperature above 180 K and $<0.030 \pm 0.003$ W m⁻¹ K⁻¹ at room temperature. The longitudinal sound speed as measured by picosecond acoustics was 2300 ± 100 m s⁻¹, 30% lower than that in C₆₀/C₇₀ fullerite compacts. Using Einstein's model of thermal conductivity, we found the Einstein characteristic frequency of microcrystalline PCBM is 2.88×10^{12} rad s⁻¹. Through a comparison of our data to previous reports on C₆₀/C₇₀ fullerite compacts, we have argued that the molecular tails on the fullerene moieties in our PCBM films are responsible for lowering both the apparent sound speeds and characteristic vibrational frequencies below those of fullerene films. In turn, the room-temperature thermal conductivities of PCBM thin films are the lowest reported of any fully dense solid.

J. C. D. and P. E. H. acknowledge funding from the National Science Foundation (CBET-1134311). Y. S. and M. C. G. would like to thank the NASA Langley Professor Program, NSF I/UCRC program, and the University of Virginia Energy Initiative for financial support. This work was supported in part by the Laboratory Directed Research and Development (LDRD) program at Sandia National Laboratories.

*phopkins@virginia.edu

†mgupta@virginia.edu

- [1] D. G. Cahill, *MRS Bull.* **37**, 855 (2012).
- [2] A. Einstein, *Ann. Phys. (Berlin)* **340**, 679 (1911).
- [3] P. Debye, *Ann. Phys. (Berlin)* **344** 789 (1912).
- [4] C. Kittel, *Introduction to Solid State Physics* (Wiley, Hoboken, New Jersey, 2005), 8th ed.
- [5] W. Kim, R. Wang, and A. Majumdar, *Nano Today* **2**, 40 (2007).
- [6] K. E. Goodson, *Science* **315**, 342 (2007).
- [7] D. G. Cahill and R. O. Pohl, *Annu. Rev. Phys. Chem.* **39**, 93 (1988).

- [8] D. G. Cahill, S. K. Watson, and R. O. Pohl, *Phys. Rev. B* **46**, 6131 (1992).
- [9] M. N. Touzelbaev, P. Zhou, R. Venkatasubramanian, and K. E. Goodson, *J. Appl. Phys.* **90**, 763 (2001).
- [10] R. M. Costescu, D. G. Cahill, F. H. Fabreguette, Z. A. Sechrist, and S. M. George, *Science* **303**, 989 (2004).
- [11] Y. S. Ju, M.-T. Hung, M. J. Carey, M.-C. Cyrille, and J. R. Childress, *Appl. Phys. Lett.* **86**, 203113 (2005).
- [12] C. Chiritescu, D. G. Cahill, C. Heideman, Q. Lin, C. Mortensen, N. T. Nguyen, D. Johnson, R. Rostek, and H. Böttner, *J. Appl. Phys.* **104**, 033533 (2008).
- [13] C. Chiritescu, C. Mortensen, D. G. Cahill, D. Johnson, and P. Zschack, *J. Appl. Phys.* **106**, 073503 (2009).
- [14] P. E. Hopkins, B. Kaehr, L. M. Phinney, T. P. Koehler, A. M. Grillet, D. Dunphy, F. Garcia, and C. J. Brinker, *J. Heat Transfer* **133**, 061601 (2011).
- [15] J. L. Lensch-Falk, D. Banga, P. E. Hopkins, D. B. Robinson, V. Stavila, P. A. Sharma, and D. L. Medlin, *Thin Solid Films* **520**, 6109 (2012).
- [16] P. E. Hopkins, B. Kaehr, E. S. Piekos, D. Dunphy, and C. J. Brinker, *J. Appl. Phys.* **111**, 113532 (2012).
- [17] J. R. Olson, K. A. Topp, and R. O. Pohl, *Science* **259**, 1145 (1993).
- [18] C. Chiritescu, D. G. Cahill, N. Nguyen, D. Johnson, A. Bodapati, and P. Zschack, *Science* **315**, 351 (2007).
- [19] Y. Shen, K. Li, N. Majumdar, J. C. Campbell, and M. C. Gupta, *Solar Energy Mater. Sol. Cells* **95**, 2314 (2011).
- [20] M. T. Rispens, A. Meetsma, R. Rittberger, C. J. Brabec, N. S. Sariciftci, and J. C. Hummelen, *Chem. Commun. (Cambridge)* 2116 (2003).
- [21] H. Hoppe and N. S. Sariciftci, *J. Mater. Chem.* **16**, 45 (2006).
- [22] D. G. Cahill, K. Goodson, and A. Majumdar, *J. Heat Transfer* **124**, 223 (2002).
- [23] C. Chiritescu, Ph.D. thesis, University of Illinois at Urbana-Champaign, 2010.
- [24] D. G. Cahill, *Rev. Sci. Instrum.* **75**, 5119 (2004).
- [25] A. J. Schmidt, X. Chen, and G. Chen, *Rev. Sci. Instrum.* **79**, 114902 (2008).
- [26] P. E. Hopkins, J. R. Serrano, L. M. Phinney, S. P. Kearney, T. W. Grasser, and C. T. Harris, *J. Heat Transfer* **132**, 081302 (2010).
- [27] P. E. Hopkins, B. Kaehr, E. S. Piekos, D. Dunphy, and C. J. Brinker, *J. Appl. Phys.* **111**, 113532 (2012).
- [28] Y. K. Koh, M.-H. Bae, D. G. Cahill, and E. Pop, *Nano Lett.* **10**, 4363 (2010).
- [29] To ensure losses to ambient did not distort our results, measurements were made with the sample both under vacuum and exposed to ambient conditions; no differences were observed.
- [30] A. J. Schmidt, R. Cheaito, and M. Chiesa, *Rev. Sci. Instrum.* **80**, 094901 (2009).
- [31] F. P. Incropera and D. P. DeWitt, *Fundamentals of Heat and Mass Transfer* (Wiley, New York, 2002), 5th ed.
- [32] C. Thomsen, J. Strait, Z. Vardeny, H. J. Maris, J. Tauc, and J. J. Hauser, *Phys. Rev. Lett.* **53**, 989 (1984).
- [33] C. Thomsen, H. T. Grahn, H. J. Maris, and J. Tauc, *Phys. Rev. B* **34**, 4129 (1986).
- [34] R. M. Costescu, M. A. Wall, and D. G. Cahill, *Phys. Rev. B* **67**, 054302 (2003).
- [35] A. J. Bullen, K. E. O'Hara, D. G. Cahill, O. Monteiro, and A. von Keudell, *J. Appl. Phys.* **88**, 6317 (2000).
- [36] W. Wang, Z. Wang, J. Tang, S. Yang, H. Jin, G.-L. Zhao, and Q. Li, *J. Renewable Sustainable Energy* **1**, 023104 (2009).
- [37] A. A. Balandin, *Nat. Mater.* **10**, 569 (2011).
- [38] J. C. Duda, P. E. Hopkins, Y. Shen, and M. C. Gupta (unpublished).